SPE SOLIDS PROCESS ENGINEERING & PARTICLE TECHNOLOGY TUHH

SPE-Schriftenreihe 18

Herausgegeben von Prof. Dr.-Ing. habil. Dr. h.c. Stefan Heinrich

Sören Ernst Lehmann

Modeling and Flowsheet Simulation of Vibrated Fluidized Bed Dryers

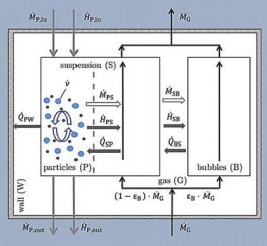

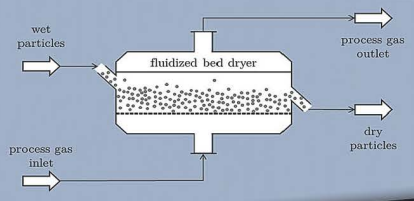

Cuvillier Verlag Göttingen
Internationaler wissenschaftlicher Fachverlag

1

Introduction

1.1 Fluidized Bed Technology

The first industrial application of fluidized bed technology was documented in Germany in 1922. The application was the production of hydrogen gas from fuel particles, suspended in a fluid-like state by a gas flow (Winkler, 1922). This fluid-like or fluidization state is reached, when gravitational and inertia forces of particles are in equilibrium with drag forces, exercised by an upwards-flowing gas. In fluidized beds, the particles are constantly in motion, resulting in high degree of mixing. Also, the porosity of the bed is increased, compared to the fixed bed state. Both lead to significantly higher heat and mass transfer between particles and fluidization gas. The mixing additionally entails homogeneous particle properties, such as temperature, moisture content, or progress of potential chemical reactions with the gas phase (Kunii et al., 2013).

Nowadays, fluidized beds are widely applied in several industrial fields, such as chemical engineering, combustion, mineral and ore processing, or pharmaceutical and food industry. Applications vary from drying purposes over chemical reactions to particle formulation. Regardless of the application, the interactions between the fluidization gas and the particles determine the properties and potential uses of the fluidized bed (Werther et al., 2014). Those interactions are summarized under the term hydrodynamics, which covers the flow of the gas in form of suspension gas and bubbles, the size, velocity and flow pattern of gas bubbles, the mixing and flow pattern of the particles as well as the resulting bed expansion, respectively bed porosity. Different flow regimes are achieved by variation of gas flow rate (Kunii et al., 2013). The most important flow regimes of gas solid fluidized beds are shown in Figure 1.1.

The fixed bed regime (A) is the regime where the gas, passing through the bed, does not apply sufficient drag to set the particles in motion. Once the drag forces on the particles are large enough to lift the particles and suspend them, minimum fluidization is reached (B). The onset of fluidization, also called minimum fluidization velocity u_{mf}, marks the theoretical lower end of the operational range of fluidized beds. When the gas velocity is increased, the pressure drop across the bed stays constant until particles are entrained

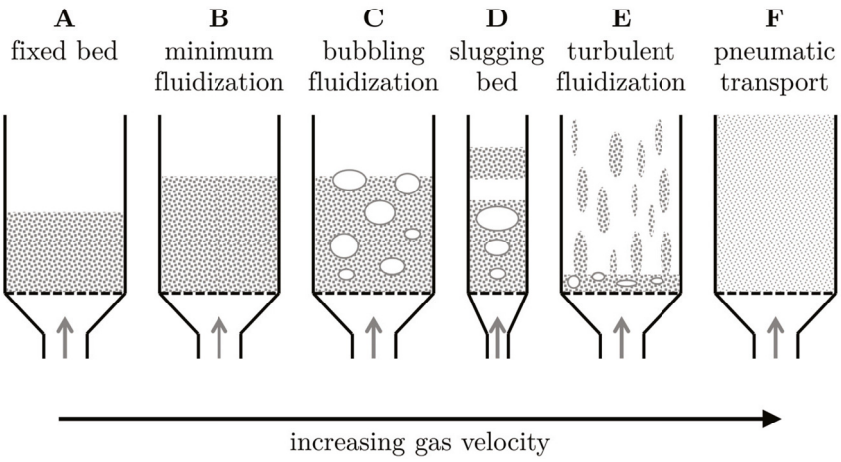

Figure 1.1: Relevant flow regimes of gas solid fluidized beds, depending on gas velocity.

from the bed. This is accompanied by expansion of the bed. Further increase in gas velocity results in the formation of bubbles. The bubbling regime (C) is accompanied by further expansion of the bed. The bubbles cause intense mixing of the particles, which results in the high heat and mass transfer rates, characteristic for fluidized beds. In case the bed is narrow, bubbles may grow as large as the cross-sectional area of the bed, resulting in slugging (D). For further increased gas velocity, the turbulent regime (E) follows. Here, the particles are moving upwards in strains or small clusters and travel downwards near the walls. The onset of particles being dragged from the bed is called the elutriation velocity u_{elu}. Operation of fluidized beds at or above u_{elu} is applied in some cases, e.g. chemical looping combustion or catalytic cracking (Kunii et al., 2013), but are beyond the scope this work and are therefore not further discussed. When the gas velocity is increased even further, pneumatic transport (F) of individual particles is achieved, the particles are carried out of the system. This work focuses on bubbling fluidized beds.

The so-called *two-phase model* is used to describe the hydrodynamics of fluidized beds. It states that the gas can be distinguished into two phases: 1) the bubbles traveling through the bed, which are mainly responsible for mixing the particles; as well as 2) the suspension gas, which is in direct contact with the particles and is thus, responsible for most of the heat and mass transfer between particles and gas (Davidson and Harrison, 1966). The behavior of fluidized beds depends on particle properties. The most common characterization was introduced by Geldart (1973). Therein, the fluidization behavior of particles is classified by the mean particle size and density difference between particles and fluidization gas, resulting in four Geldart groups. Molerus (1982) refined Geldart's empirical findings by investigating the boundary regions between different Geldart groups. He defined the boundaries between the groups based on force

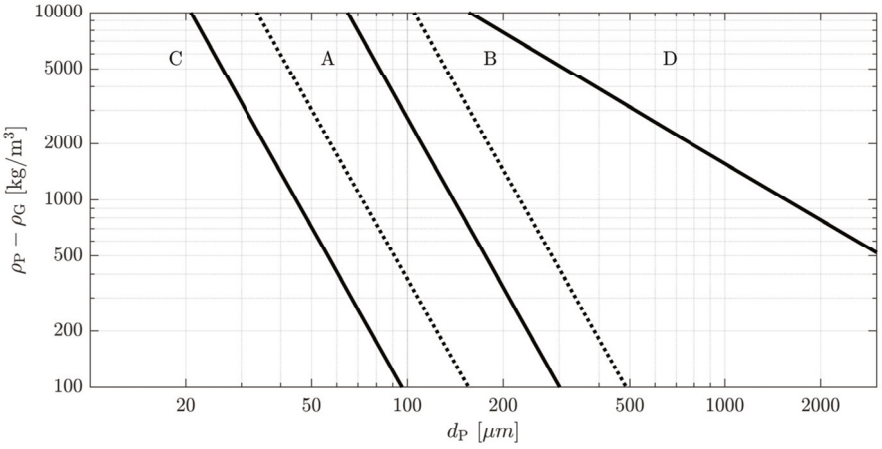

Figure 1.2: Molerus diagram, showing Geldart groups based on particle properties and respective boundaries, derived by force balances. Solid lines depict boundaries for hard particles, dashed lines indicate boundaries for softer particles, showing higher interparticle cohesiveness, according to Molerus (1982).

balances, accounting for van der Waals forces, cohesiveness due to particle hardness and the drag force exerted by the fluidization gas. The classification of powders in Geldart groups after Molerus (1982) is shown Figure 1.2.

Fluidized beds of Geldart group A expand at u_{mf} before bubbling occurs with increasing gas velocity. The bubbles are categorized as fast bubbles, because they move faster through the bed than the suspension gas. Given sufficient bed height, an equilibrium between growth and splitting of bubbles is reached, leading to a maximum bubble size. The bed collapses slowly when the gas stream is suddenly turned off (Geldart, 1973).

Group B particles have larger mean diameters and densities than group A particles. Bubbling starts immediately at u_{mf}. The bubbles also travel faster than the suspension gas. However, the bubble size does not reach an equilibrium. Bubble growth in the bed is only limited by the apparatus walls. Thus, slugging of the bed can occur with group B particles. When the gas flow is interrupted suddenly, the bed collapses immediately. The expansion of the bed is less pronounced, compared to group A powders (Geldart, 1973).

The largest and most dense particles are categorized in group D. These particles tend to form spouts and are ideal to be processed in spouted beds. When processed in a conventional fluidized bed, the bubbles move slower than the suspension gas ('slow bubbles'). The bed expands even less than group B particles and also collapses immediately after interrupting the gas flow (Geldart, 1973).

Particles of group C show small diameters (few µm or less) and are difficult to fluidize because of strong interparticle cohesion forces. Van der Waals forces in the size range of

group C particles are in the order of magnitude or larger than the gravitational forces and thus, dominate the behavior in fluidized beds. This results in the formation of agglomerates and channeling during fluidization, or the fluidization of Geldart C powder is not possible at all without assistance to overcome the cohesive forces (Geldart, 1973, Kunii et al., 2013).
For nano-particles it was observed, that fluidization is possible without assistance, but at gas velocities much higher than expected for the primary particles. This is due to the formation of dynamic agglomerates which constantly form, fall part and reform during fluidization. This phenomenon is also called aggregate-fluidization or agglomerate fluidization. Two types of agglomerate fluidization are distinguished. One is the agglomerate particle fluidization (APF). It is accompanied with a large expansion of the bed as soon as the gas flow is introduced into the bed. This bed expansion already occurs well before the fluidized bed state is achieved (Nam et al., 2004, Raganati et al., 2018). The other type is called agglomerate bubbling fluidization (ABF), which is characterized by a much lower bed expansion (compared to APF) and the occurrence of bubbles as soon as u_{mf} is reached (Gündoğdu and Tüzün, 2006, Raganati et al., 2018). However, the fluidization of nanoparticles exceeds the scope of this thesis. Thus, it is only mentioned here for the sake of completeness.

1.1.1 Drying in Fluidized Beds

'Drying' generally describes the removal of moisture from solids (Tsotsas and Mujumdar, 2011). Drying on industrial scale is widely applied, e.g. to reduce transportation costs by reduction of mass, increase shelf live of food and pharmaceutical products or achieve desired properties or functionalities. This thesis focuses on drying of particulate solids in fluidized beds. The drying process of a bulk of porous solids in fluidized beds, or a single porous particle in an air stream, is divided into characteristic drying phases or drying periods (DPs): a) the warm up phase, b) the first drying period (1st DP) and c) the second drying period (2nd DP) (Mujumdar and Devahastin, 2003). The respective periods are shown exemplary in Figure 1.3.
The warm up period is a short phase at the beginning of the drying process. Herein, the particle is warmed up to the wet bulb temperature T_{wb} and some moisture is evaporated simultaneously. Point A in Figure 1.3 marks the end of the warm up period and the beginning of the first drying period. Here, the entire particle surface is covered with water. Hence, evaporation kinetics are solely determined by gas side properties, such as temperature, flow rate and inlet moisture content of the drying gas. Therefore, the particle surface temperature as well as the temperature inside the particle equals T_{wb}. The evaporation of water takes place at a constant rate. Thus, the first drying period is also called 'constant rate period' (Tsotsas et al., 2000).
The evaporation rate is reduced, when the particle surface is not completely covered with water. This point (B) marks the transition to the second drying period. As a consequence, the particle surface is in direct contact with the drying gas, resulting in

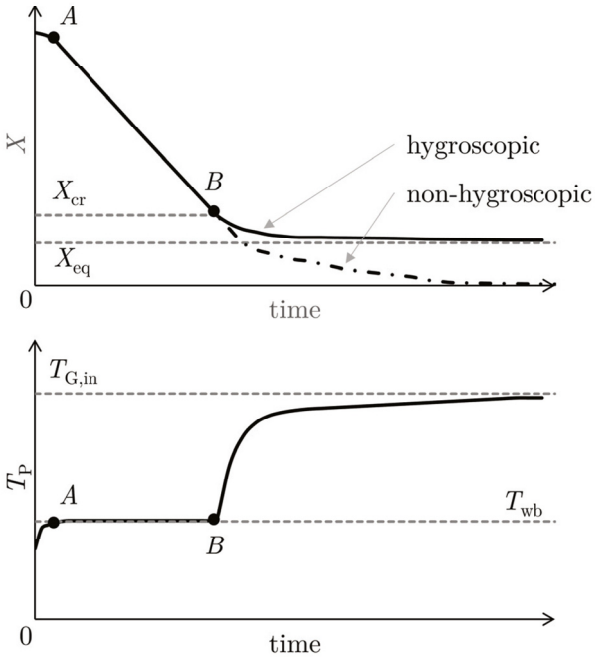

Figure 1.3: Exemplary course of drying of porous particles in fluidized beds, showing particle moisture content (X) and particle temperature (T_P) against time, (top) and (bottom) respectively; including transition points between drying periods.

heating of the particle. In the second drying period or 'falling rate period', intraparticle transport phenomena determine the overall drying rate. These are transport of liquid water and diffusion in pores and capillaries. Simultaneous heating of the particle as well as potential changes of pore size, structure or tortuosity are superimposed and influence each other. The ultimate consequence is asymptotic approach of particle temperature towards the inlet gas temperature with passing time. Simultaneously, particle moisture content approaches the equilibrium moisture content. The equilibrium between particle moisture content and drying gas is zero for non-hygroscopic materials. The majority of porous particles are hygroscopic, meaning that the equilibrium moisture content is larger than zero, as long as the drying gas is not entirely free of moisture at the inlet (Tsotsas et al., 2000).

Due to the complexity of the involved physics in the second drying period, modeling of this period is challenging. Several approaches have been proposed and investigated. A detailed review of drying kinetics in fluidized beds and respective modeling approaches is conducted in chapter 2.2.

1.1.2 Assisted Fluidization

Many products, produced by fluidized bed drying, have small particle sizes (Geldart groups A and C) (Mawatari et al., 2015) or exhibit cohesive behavior due to their chemical composition (e.g. amorphous lactose) (Palzer, 2005, Pisecký, 2012). The presence of water during drying processes poses an additional source of potentially strong cohesive forces. As discussed above, fluidization of cohesive powders is often hindered by channeling (rat holes) and formation of agglomerates or stagnant regions in the bed. Several methods have been identified to improve fluidization in the mentioned cases. Such methods are pulsation of air flow, introduction of acoustic or mechanical vibration, magnetic or electric fields, modification of internals (i.e. baffles, agitators) or combinations of the aforementioned. The common purpose of all these approaches is counteracting cohesive forces by introduction of additional forces. Thereby, the target is to improve, or in some cases, enable fluidization, by reducing agglomeration and channeling (van Ommen, 2009).

Mechanical vibration of the fluidized bed apparatus is the option, which is most commonly applied on industrial scale for fluidized bed drying (Pisecký, 2012). As such vibrated fluidized beds are common in the food and pharmaceutical industry, they have been object of many investigations (Brennan et al., 2008, Gupta and Mujumdar, 1980, Jia et al., 2015, Kage et al., 1999, Kósa and Verba, 2001, Mawatari et al., 2015, 2003, Wang et al., 2000). The intended goal is to overcome interparticle forces by added vibration energy. This results in breakage of agglomerates and channels, respectively the reduction of cohesiveness. The vast majority of experimental research has been preformed in lab-scale fluidized beds with diameters ranging between a few centimeters and a couple of decimeters, or in pseudo two dimensional beds. Vibration of fluidized beds is generally reported to result in enhanced or improved fluidization. This means in particular reduction of u_{mf}, increase of bed pressure drop and bed expansion. Furthermore, a decrease in channeling was observed with increasing vibration. Another general observation is, that the effect of vibration is stronger for Geldart group C particles than for group A and B (Mawatari et al., 2015, Xu and Zhu, 2006).

In other cases, vibration was found necessary to enable fluidization of cohesive powders in the first place (Gupta and Mujumdar, 1980, Noda et al., 1998). Furthermore, Xu and Zhu (2005) observed that segregation (of smaller agglomerates at the top and larger agglomerates at the bottom of a fluidized bed) could be reduced by vibration. Reduced segregation, respectively better mixing in VFBs, was also reported by Lee et al. (2020).

The strength of vibration is often expressed as the dimensionless vibration number, which is defined as the ratio of acceleration due to vibration and gravitational acceleration:

$$\Lambda = \frac{(2\pi \cdot f)^2 \cdot A_{\mathrm{vib}}}{g} \,. \tag{1.1}$$

Therein, f is the frequency, A_{vib} the amplitude of vibration and g the acceleration due to gravity. The sole characterization of vibration effects with Λ is questionable, because different combinations of frequency and amplitude can result in the same value of Λ. It was shown, that significant differences in fluidization behavior resulted for constant Λ, but for different combinations of f and A_{vib}. Thus, amplitude and frequency should always be considered individually (Daleffe et al., 2005, Meili et al., 2012).
Besides frequency and amplitude, the direction of vibration affects the fluidized bed (Mawatari et al., 2001). Xu and Zhu (2006) investigated different angles of vibration. For glass beads, their results show that horizontal vibration leads to lower u_{mf} with increasing frequency, whereas vertical vibration results in lower u_{mf} for lower frequencies. Accurate modeling of such effects is a key aspect of this thesis and an important part in the proposed flowsheet simulation model for vibrated fluidized bed dryers. The effects of vibration on hydrodynamics and drying kinetics in fluidized beds are elucidated in more detail in chapter 2.1.3.

1.2 Flowsheet Simulation of Solids Processes

Flowsheet simulation tools have been developed since the late 1970s. Their primary goal is the simulation of process chains, consisting of different unit operations. Key applications of flowsheet simulation are a) modeling of process behavior, b) sensitivity analysis, c) process optimization and d) process control. The vast majority of the underlying models are of empirical or semi-empirical nature. This macroscopic modeling approach allows for simulation of large time scales of complex and interconnected process chains in reasonable computational time (Gleiss et al., 2017, Puettmann et al., 2012).
The original focus lay on liquid and gas phase processes, allowing for the description of the phase properties by bulk parameters, which are often thermodynamic parameters. The detailed description of particulate materials requires consideration of interdependent multidimensional distributed parameters (Dosta et al., 2020, Skorych et al., 2020). In the example of drying, the moisture content changes. This entails simultaneous change in density and potentially changes in temperature, surface composition or size. The resulting systems of partial and ordinary integro-differential equations require special solvers and data handling algorithms (Skorych et al., 2019). Some commercial flowsheet simulation packages are nowadays available for solid processes, such as Aspen Plus (*Aspen Technology Inc.*), JKSimMet (*JKTech Pty Ltd.*), gPROMS Formulated Products (*Process Systems Enterprise Ltd.*) or CHEMCAD (*Chemstations Inc.*). An open-source alternative is the framework DYSSOL. It was developed specifically for solid processes, within the DFG priority program SPP 1679 (Heinrich, 2020, Skorych et al., 2020). It allows for steady-state and time-dynamic flowsheet simulations and is used in the scope of this work.
DYSSOL is based on the sequential-modular approach. This allows for the application of different solution approaches in different units, which is highly advantageous when

units with different multidimensional population balance models need to be solved. The waveform relaxation approach is used to increase efficiency in data transfer between units and improve convergence of the flowsheet (Skorych et al., 2020). In the DYSSOL framework, transformation matrices are used for the calculation of the multidimensional distributed parameters. Implicit calculation of transformation matrices for every unit model allows for the efficient calculation of holdups and input/output streams for the combination of process units (Skorych et al., 2019, 2017).

1.3 Objectives and Strategy

Drying is an important but very energy intensive process. Thus, even small improvements may lead to substantial savings in energy and costs. Fluidized bed drying is the prime choice when heat sensitive product need to be dried, which are very common in the pharmaceutical and food industry. As many products in these industries are fine and cohesive, mechanical vibration of the dryer is used to enable or improve fluidization. As fluidized bed drying is often one of many unit operations in industrial production processes, flowsheet simulation is a powerful tool for investigation and optimization of entire process chains. However, all unit operations must be modeled accurately and with reasonably low computational demand, respectively computational time. Thus, quality and robustness of the underlying model equations are paramount.
Fluidized bed drying has been investigated intensively for decades. A number of models has been proposed, of which only a few are available in flowsheet simulation frameworks. These models are sometimes only tested for a small range of process parameters and particles of only one Geldart group (Alaathar, 2017, Alaathar et al., 2020), despite significant differences and resulting deviations. Others suffer from constraints imposed by the simulation framework, e.g. that distributed material properties cannot be considered. Furthermore, the influence of vibration is not yet included in established models. Thus, the goal of this thesis is the development of a fluidized bed drying model that covers the influence of mechanical vibration of the dryer and its implementation in an open-source flowsheet simulation framework. The model is tested for a variety of particles, belonging to different Geldart groups, as well as varied dryer geometries and ranges of process conditions related to food and pharmaceutical industry. Therefore, models of fluidized bed hydrodynamics need to be developed, accounting for the impact of vibration and residence time distribution of particles, in dependence of process parameters and dryer geometry. Suitable semi-empirical correlations are identified by comprehensive experimental parameter studies.
The newly developed model parts are combined with established and reliable models and implemented in the open source flowsheet simulation framework DYSSOL. During the model development and implementation, the focus lies on the broadest possible application range of the model. Thorough validation with experimental data and sensitivity analysis are conducted to prove accuracy and reliability of model predictions, confirm

underlying assumptions and identify potential weak points as well as optimization parameters.

1.4 Outline of the Thesis

This thesis covers experimental investigations for the development as well as validation of a flowsheet simulation model for vibrated fluidized bed dryers. In chapter 2 modeling approaches for fluidized bed hydrodynamics, particle residence time distribution and drying kinetics are reviewed. Suitable model correlations are identified alongside areas that require further research. Furthermore, corresponding experimental investigation techniques are introduced and discussed.
Chapter 3 contains the experimental methodology of the thesis. The investigated materials are characterized with regard to properties, relevant in fluidized bed drying and the respective measurement procedures are introduced. This is followed by a detailed introduction of the different fluidized bed dryers and the installed measurement equipment, as well as specifics about the experimental procedures, used in the scope of this work.
The discussion and interpretation of experimental results is divided into two parts. Chapter 4 is concerned with the development of suitable correlations to accurately model fluidized bed hydrodynamics under the influence of vibration as well as for fine and cohesive particles. Additionally, residence time characteristics are investigated experimentally and the results are included into the model. Modeling of material specific drying kinetics of the investigated powders follows as the third pillar of the model. Lastly, the developed model and underlying assumptions are introduced in detail, the chosen correlations are discussed and the implemented structure of the different model parts is established.
The model performance is thoroughly explored in chapter 5. Model predictions are validated by comparison to experimental data. A wide range of process parameters and particles of different Geldart groups is tested, as well as the influence of different dryer geometries and vibration on the drying process and model predictions. Subsequently, crucial assumptions and model stability are examined. Additionally, sensitivity analysis with respect to process parameters is conducted. Potential fitting parameters are identified and the overall model performance is evaluated.
Concluding remarks are made in chapter 6. Here, the thesis is summarized, key findings are highlighted and topics for further research and options for continued development of this fluidized bed drying model are pointed out.